



**HAL**  
open science

# TFM imaging simulations of defects near or in the weld bevel: modelling approach and advances on new hybrid finite element tools

Nicolas Leymarie, Alexandre Imperiale, Jordan Barras, Edouard Demaldent

## ► To cite this version:

Nicolas Leymarie, Alexandre Imperiale, Jordan Barras, Edouard Demaldent. TFM imaging simulations of defects near or in the weld bevel: modelling approach and advances on new hybrid finite element tools. e-Journal of Nondestructive Testing, 2023, 28 (10), pp.28707. 10.58286/28707 . cea-04222479

**HAL Id: cea-04222479**

**<https://cea.hal.science/cea-04222479>**

Submitted on 29 Sep 2023

**HAL** is a multi-disciplinary open access archive for the deposit and dissemination of scientific research documents, whether they are published or not. The documents may come from teaching and research institutions in France or abroad, or from public or private research centers.

L'archive ouverte pluridisciplinaire **HAL**, est destinée au dépôt et à la diffusion de documents scientifiques de niveau recherche, publiés ou non, émanant des établissements d'enseignement et de recherche français ou étrangers, des laboratoires publics ou privés.



Distributed under a Creative Commons Attribution 4.0 International License

## **TFM imaging simulations of defects near or in the weld bevel: modelling approach and customized finite element tools**

Nicolas LEYMARIE<sup>1</sup>, Alexandre IMPERIALE<sup>1</sup>, Jordan BARRAS<sup>1</sup>,  
Pierre-Emile LHUILLIER<sup>2</sup>, Andreas SCHUMM<sup>2</sup>, Yann GELEBART<sup>2</sup>,  
Edouard DEMALDENT<sup>1</sup>

<sup>1</sup>Université Paris-Saclay, CEA, List, F-91120, Palaiseau, France

<sup>2</sup>EDF R&D, EDF Lab Les Renardières, Département Matériaux et Mécanique des Composants, 77818 Moret-sur-Loing, France

### **Abstract**

In safety-critical industries, including the nuclear sector, ultrasonic testing (UT) of welded components is an area of continuous improvement. We have collaborated on developing advanced UT simulation tools to address challenges in monitoring and imaging defects near or within a weld bevel. These tools, integrated into the CIVA software platform, use hybrid approaches combining ray models and finite elements (FE) to accurately simulate wave propagation and diffraction phenomena in both 2D and 3D inspection configurations. While computation time is longer compared to ray-based approaches, the results serve as a reference for improving reliability and validating simulation tools. A comprehensive parameterization of the weld is proposed, utilizing knowledge on anisotropy, attenuation properties, and variations within the bevel, to achieve reliable UT results. This paper reviews the new features developed, including the integration of the MINA model for the weld description and improvements in bevel geometry. The automated coupling methodology and meshing procedures, which do not require any specific numerical expertise to be used, are discussed. As an application, we present TFM imaging simulations, comparing results from the standard paraxial ray-based approach with the new module utilizing the FE computational core.

**Keywords:** UT simulation, weld modelling, anisotropy, MINA-like description, TFM imaging

## **1. Introduction**

Safety-critical industries, particularly the nuclear sector, are subject to extremely stringent safety regulations. Nuclear power plants rely on various welded structures, such as pressure vessels and piping systems, which are exposed to harsh environments and require regular inspections. Ultrasonic testing (UT) is a valuable technique used to inspect these welded components, as it enables in-depth non-destructive evaluation by allowing elastic waves to penetrate materials like steel. The emergence of phased array technology (PAUT), specifically TFM/FMC or PWI imaging techniques [1], [2], has led to their increasing adoption. These techniques provide detailed images and can detect and size potential defects. However, when applied to the inspection of welded areas, the complexity of these new PAUT imaging techniques is combined with the complexity of the components themselves. Welded areas often have irregular and chaotic geometries, as well as local anisotropic and heterogeneous properties, especially when considering austenitic steel welds. Consequently, ultrasound responses can include numerous indications that are challenging to analyse and classify.

Thus, having access to high-performance and accurate simulation tools is crucial for a better understanding of the phenomena involved. UT simulation tools are increasingly used to explain the behaviour of ultrasonic waves in situations where elastic materials and/or geometries become non-trivial. In proof-of-performance demonstrations, simulation tools offer numerous advantages, including the integration of sensitivity analysis on uncertain parameters [3]. This capability allows for improved detection performance and the prediction of UT signals in

scenarios that are difficult to set experimentally [4], [5]. As a result, the implementation of new UT techniques can be expedited while reducing associated timeframes and costs. It is then essential to provide flexible simulation tools that facilitate parametric studies. This can be accomplished by offering numerical models specifically tailored to typical industrial scenarios. To meet this need, teams from EDF R&D and CEA List have collaborated to develop solutions using parametric descriptions close to industrial data to take into account the specific features of austenitic weld components:

- dissimilarities in the bevel geometries observed in relation to the nominal description,
- the variations in anisotropy associated with welding processes and grain growth orientations using the MINA modelling approach [6],
- the branched crack geometries commonly encountered in stress corrosion defects.

Integrated within the CIVA NDT simulation software platform, a particular effort has been made to obtain comprehensive parametric descriptions of the weld with relevant parameters. Taking advantage of the work already carried out on the CIVA asymptotic ray models applied to smoothly inhomogeneous weld properties [7]–[9], we have developed a new hybrid FE solution which allows us to model the ultrasonic interactions within the component using only an FE calculation kernel. The objective here is to be able to provide a reference solution to the non-expert user to qualify or not other simulation results produced using models that are faster but subject to additional approximations that may lead to numerical artefacts. Such artefacts are sometimes non-negligible and difficult to apprehend a posteriori.

In the first part, we present in more detail the different possibilities for defining the variability of the properties of the welded zone, both in terms of its geometry and its material properties. We then describe the calculation kernels available in CIVA for simulating UT methods on these welds, with particular emphasis on the new hybrid solutions based on an all-FE calculation in the part. Finally, we illustrate our statements using a representative application case for the simulation of TFM/FMC imaging procedure.

## **2. Parametric weld descriptions for UT simulations in CIVA**

CIVA is best known for its simulation capabilities oriented towards a very broad parametric description (sample, probe, material properties, defects, delay laws ...). It enables users to create virtual components, define inspection parameters and simulate the behaviour of various existing or original UT methods. In the case of austenitic welds for stainless steels, it is very useful to model the welded zone as accurately as possible in order to understand the possible wave interactions between the geometry of the chamfer, the properties of the weld and the defects located in this region.

### ***2.1 Bevel and assembling surface geometries***

The "weld" type part model in CIVA is defined as a parametric 2D CAD incorporating the geometry of the chamfer between the two butt-welded components, the thickness of which is defined. The 3D geometry of the component is then defined as a rectilinear or circular extrusion of this profile. The chamfer geometries available include all the standard chamfers used in existing welding processes, as well as more generic models that can be adapted to mock-up configurations deformed from their nominal state (see Figure 1).

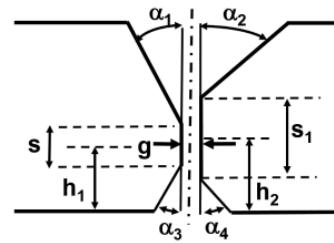
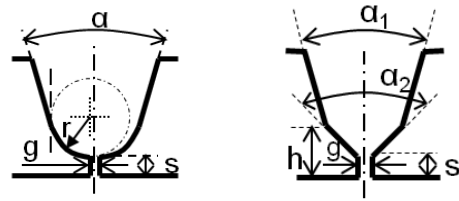
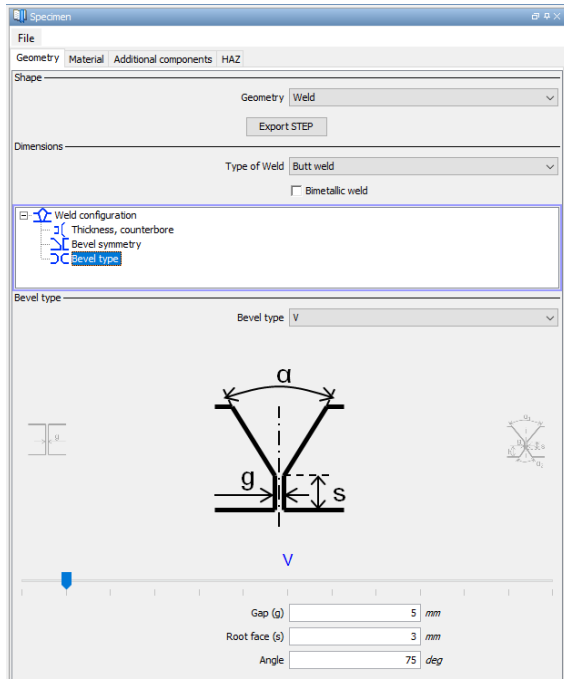


Figure 1: Features of the CIVA GUI for defining various bevel geometries

In addition, other geometric specificities can be added, such as cladding, but also geometric deformations on the surface or on the backwall of the part corresponding to slopes linked to counter-boring processes (see Figure 2).

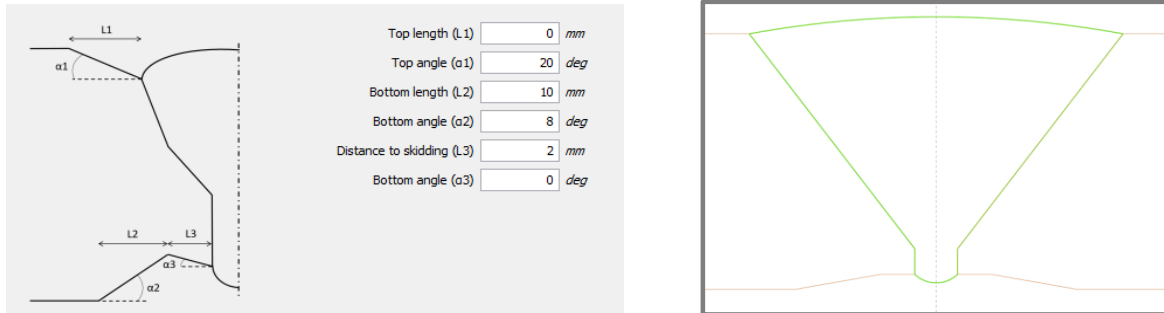


Figure 2: New specific settings to define geometry changes to the top and bottom of the welding component in the connection area with the bevel.

## 2.2 Advanced material properties for austenitic welds

The simulation of UT inspection of welding structures requires a good knowledge of the geometry but also of the mechanical properties attributed to the weld. In practice, it is unrealistic to define a detailed microstructure of the material of the welded part. To model the effects of the microstructure on the coherent wavefront of the ultrasonic beam, we typically use effective material properties that correspond to an anisotropic damped material. Due to its columnar grain microstructure textured around the grain elongation axis, the symmetry of austenitic weld material is considered to be quasi-hexagonal, with a symmetry axis correlated to the main elongation axis. In the following simulation results, we assume to define such macroscopic behaviour with the help of a complex-valued stiffness tensor (see Table 1).

Effective stiffnesses (GPa)	$C_{11}$	$C_{22} = C_{33}$	$C_{12} = C_{13}$	$C_{23}$	$C_{44}$	$C_{55} = C_{66}$
<b>Real Part</b>	220	245	135	110	80	110
<b>Imaginary Part</b>	1.6	12	2	2.5	2.7	4.3

Table 1. Complex stiffness coefficients used for effective austenitic weld properties inspired from [10].

Austenitic welded material microstructure obtained with Shielded Metal Arc Welding (SMAW) can vary within the chamfer depending on welding process. These variations can be modelled in general either by a piecewise description, or with the help of continuously variable orientation maps. In order to assist the user in defining such inputs, the MINA model (Modelling anisotropy from Notebook of Arc welding) co-developed by EDF [6] is now integrated into CIVA using specifications linked to the deposit process (number of passes, order in which the passes are applied as illustrated Figure 3).

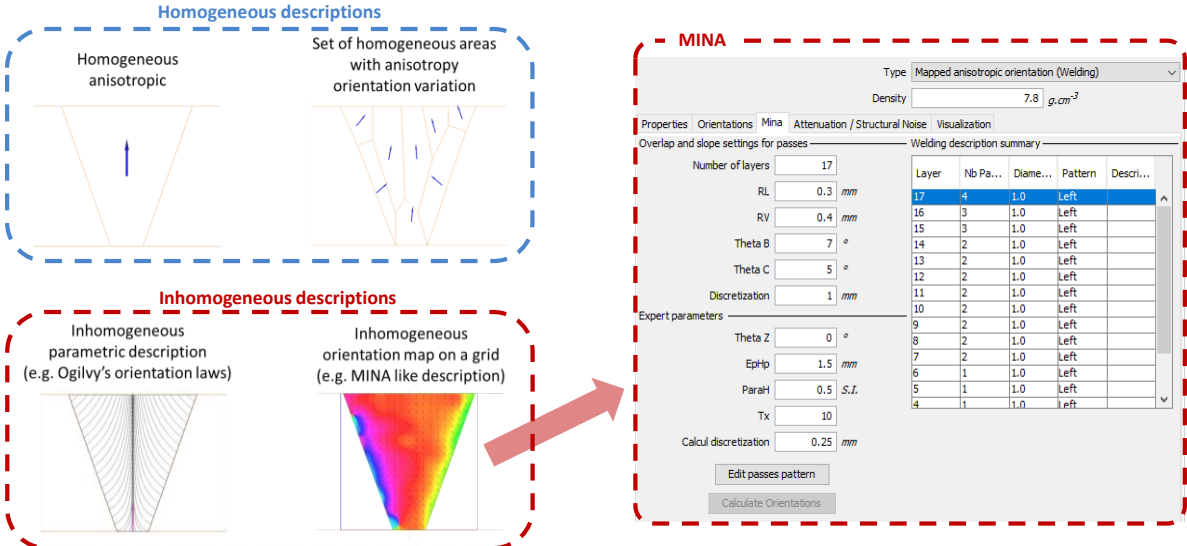


Figure 3: Commonly used models for grain orientation descriptions within the bevel and the MINA panel recently implemented in CIVA to generate orientation map.

### 2.3 Realistic crack geometries

The last part concerns the definition of a complex-shaped defect imitating the shape of a stress corrosion cracking (SCC), which often has a multiple ramification. These can be represented in CIVA using extruded 2D CAD, the latter being defined using the mesh of a deformed grid, certain edges of which are tagged as a defect part and ultimately correspond to interfaces for which free boundary conditions are considered (see example Figure 4).

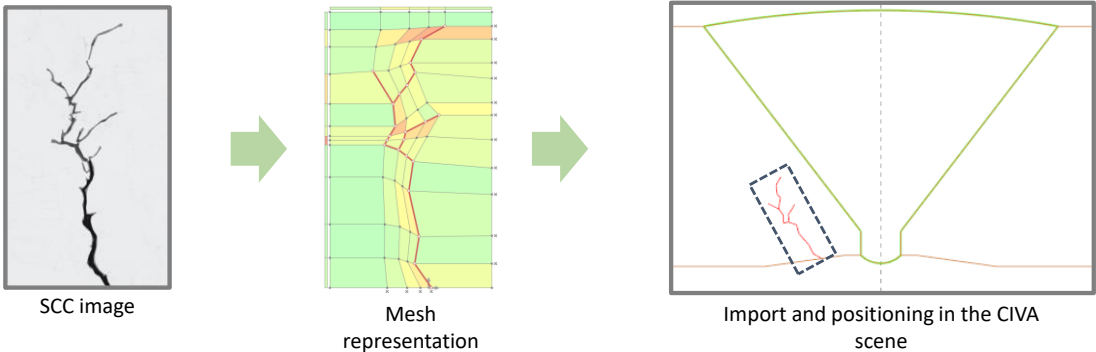


Figure 4: Parametric description of defects to represent stress corrosion cracking in CIVA: the original image, its representation in a deformed mesh grid and its positioning in the welding part.

For example, we can try to fit the geometry of the defect according to a macrographic picture. The nodes associated with the defect geometry can then be moved randomly to perform some variation analysis and quantify the influence of the geometry perturbations for a given simulated testing scenario containing uncertain parameters.

### **3. Modelling approaches for UT in welding component**

In the given context, we focus on a modelling framework where the weld bevel material is considered smoothly inhomogeneous and anisotropic. When dealing with complex and heterogeneous parts, such as butt-welded components, two main families of models emerge. The first family concerns semi-analytical ray-based approaches that utilize a high frequency (HF) approximation and modal decomposition of the solution to the elastodynamics wave equation. The second family encompasses finite element (FE) or finite difference numerical methods, widely used in engineering.

The main challenge is to create customized solutions for simulating the propagation of bulk waves in three-dimensional structures while minimizing computational costs and memory usage. Ray models are known for their efficiency, but they can still produce notable quantitative errors. On the other hand, numerical models offer excellent error control but are computationally expensive, especially for 3D simulations. Hence, there is a significant interest in offering both aspects of these simulation tools. This would allow for intensive calculations using ray approaches while providing the option to assess model biases through reference solutions obtained from numerical methods.

#### ***3.1 Evolution of the modelling strategies available in the future CIVA version***

Already available in the current commercial CIVA version, the ray-based approach applied for weld orientation map descriptions is an adaptation of the pencil method [11], where the straight ray tracing in homogeneous parts is replaced by calculations of curved ray paths. This technique was initially applied for curved composite laminates [12] and then improved for austenitic weld material defined with grain orientation variations [8]. This model is much more relevant to the development of imaging techniques exploiting the properties of the coherent wavefront and the implementation of modal time-of-flight mapping as for TFM imaging. In this way, we reduce the artefacts of HF ray model generally obtained with piecewise descriptions with coarse homogeneous domains of grain orientation (see e.g. [13]). The calculation cost of these curved ray trajectories increases particularly in 3D. In fact, this requires the implementation of an iterative scheme to determine the ray propagation, whereas its cost is virtually zero for a homogeneous medium. Even if this reduces artefacts, there are still some HF singularities linked to spatial variations in the properties of the weld, and more particularly the singularities linked to caustics.

As latter mentioned, to check the impact of the HF approximations, a second option is to use numerical models, particularly FE methods, the only ones that can be adapted to inhomogeneous media and non-regular geometries. Therefore, in the next version of CIVA, we propose to simulate wave propagation in the part using only a transient spectral FE method. By combining high-order finite element basis functions with a lumped mass technique and an optimised mesh structure, we obtain an efficient FE solution with a small memory footprint compared with other standard finite element codes [14], [15]. Already implement in recent CIVA simulation modules (guided waves [16], coupling for local defect diffraction [17]), we have leveraged several enhancements to the calculation kernel, specifically addressing variable anisotropy and attenuation related to curved composite applications [18]. These improvements have enabled us to adapt these FE techniques to weld part features and add a new hybrid technique coupling ray and FE models.

#### ***3.2 Principles of the FE hybrid solutions for beam radiation and echo response***

In practice, the principle of coupling for beam calculation is straightforward. Suitable for both immersed and wedge probes, the radiated fields outside the part are estimated with the ray model and the simulation of elastic wave propagation inside the part is carried out by our FE kernel. Hence, the ray field is used as a source field for the FE computation given as a boundary condition on the surface of the component exposed to the transmitter. The FE computation

accounts for the interaction between the emitted ultrasonic wave and the inspected structure, producing simulated waveform evolution as in Figure 5.

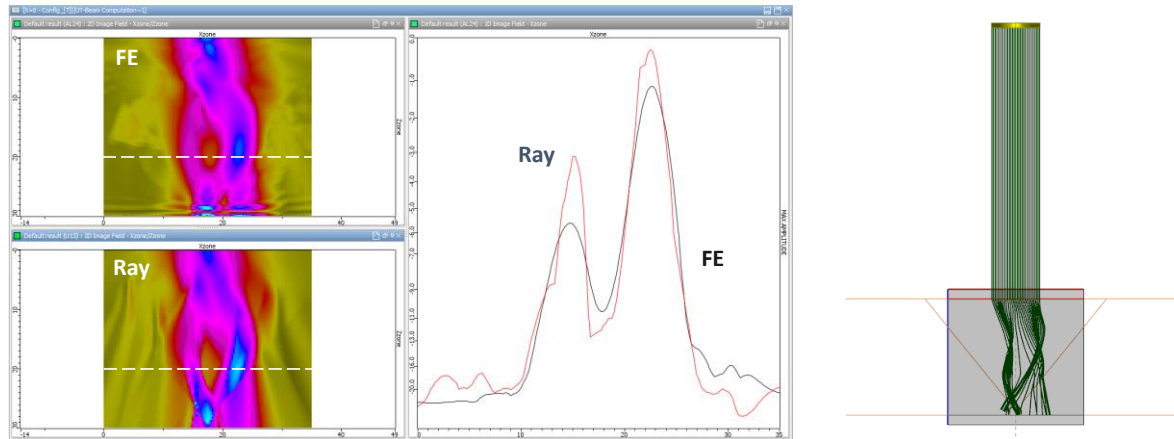


Figure 5: Comparison of the results of calculating the ultrasonic field above the weld bevel using the two modelling approaches: differences near wavefront folding caustics and echodynamic curves at 20 mm depth.

In the case of a UT simulation where we are trying to determine the ultrasound signal received by a probe, we simply need to capture the FE solution on the surface exposed to the receiver and applied the reciprocity principle as proposed in [17]. When simulating a full matrix capture (FMC) acquisition, a FE computation is conducted for each emitted shot and subsequently, elementary A-scans are determined for all receiving elements. This process involves performing individual calculations for each element in the reception array. The elementary A-scans represent the response of each receiving element as a function of time, providing information on the detected echoes received by the array probe. This step allows for the reconstruction of the complete FMC dataset, which can then be further analyzed and processed for various inspection purposes like TFM.

The main challenge lies in effectively controlling and automating the meshing and coupling procedures according to the variety of cases to be processed. Based on the macro-element (ME) decomposition strategy explained in [15], the specific meshing requirements will depend on factors such as the geometry of the weld, the position of the probe(s), and the control mode being employed (such as pulse-echo or pitch-catch techniques). By way of illustration, we give an example of a standard decomposition of the FE scene in the case of a welding component including a CSC near the bevel (see Figure 6). In the case presented, the control corresponds to pulse-echo inspection with a contact wedge probe, the coupling interface is defined close to the surface of the component at a distance of one wavelength. In addition, a thin layer of fluid coupling is considered between the wedge and the part, using low-order finite elements in the thickness direction so as not to penalize the FE time step imposed by the CFL condition. In this particular case, the calculations are penalized by the geometry of the defect and by the transverse wave velocities in the Rexolite material.

Automating these procedures ensures consistent and efficient analysis in different scenarios without requiring mesh expertise from the user. This enables accurate and reliable results to be obtained in studied non-destructive testing applications, including components with welds.

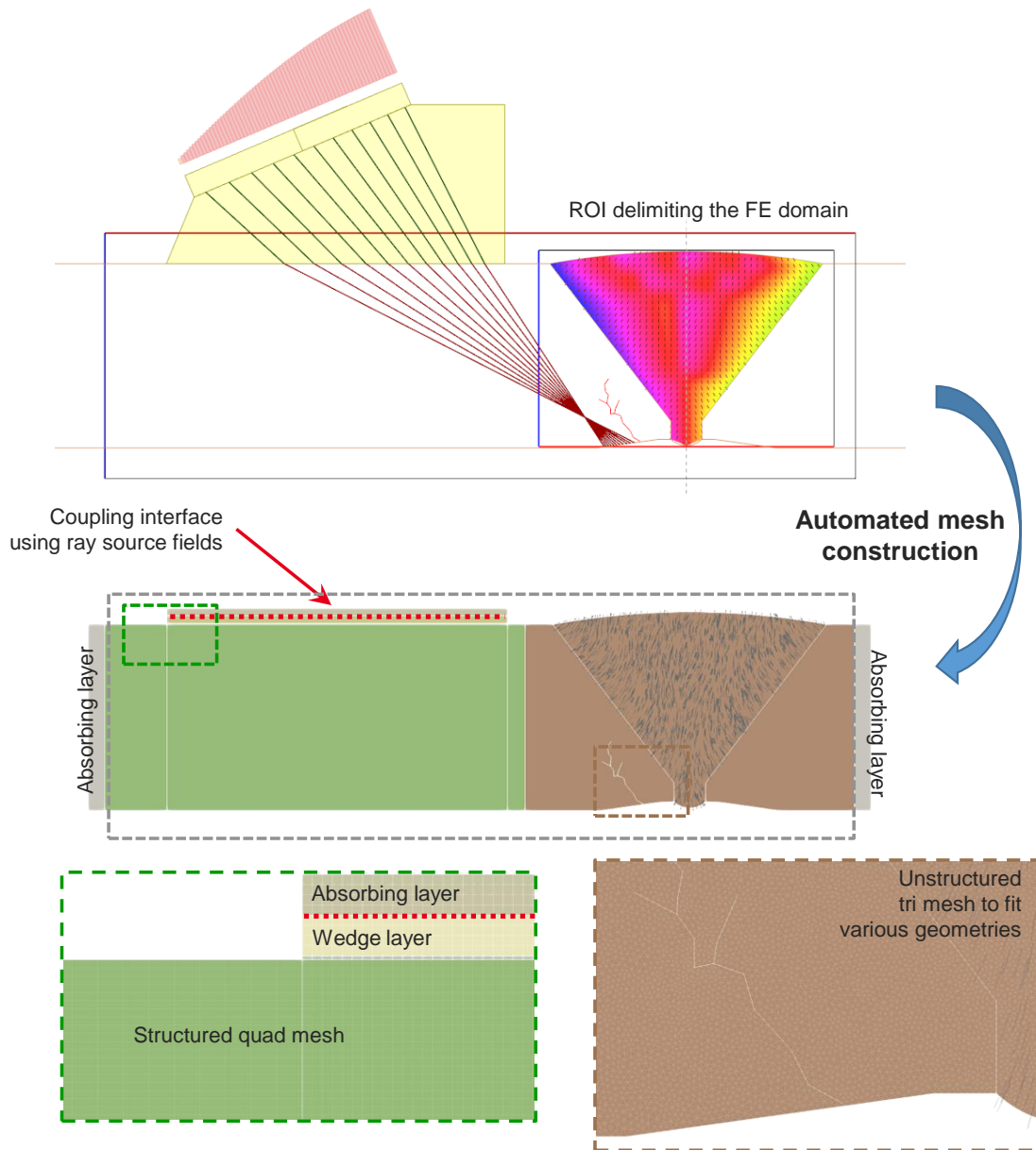


Figure 6: Example of automated mesh construction used to perform an FE calculation with an unstructured triangular mesh in the area around the bevel and structured quadrangular parts elsewhere if possible.

#### 4. TFM simulation results

In the numerical example following, we have considered a 64-element linear phased-array probe with a L60 wedge. The central frequency is fixed at 2.25 MHz with a pitch of 0.6 mm and an aperture of 38.4 mm. In order to simulate a FMC acquisition, we have to compute elementary A-scans for each of emitted element, and therefore to perform 64 FE calculations. Note that for all the next TFM imaging results, we consider a homogeneous isotropic part for the three different direct modes LL TT and LT.

As an example, we compare here only full FE simulations for a defect positioned before and in the bevel in order to estimate the effect of the weld material description on simulation results. To do this, we define three types of description: one where the component is homogeneous and isotropic and the two others where the weld is an anisotropic material with an orientation map, one without attenuation and the other with attenuation phenomena taken into account.



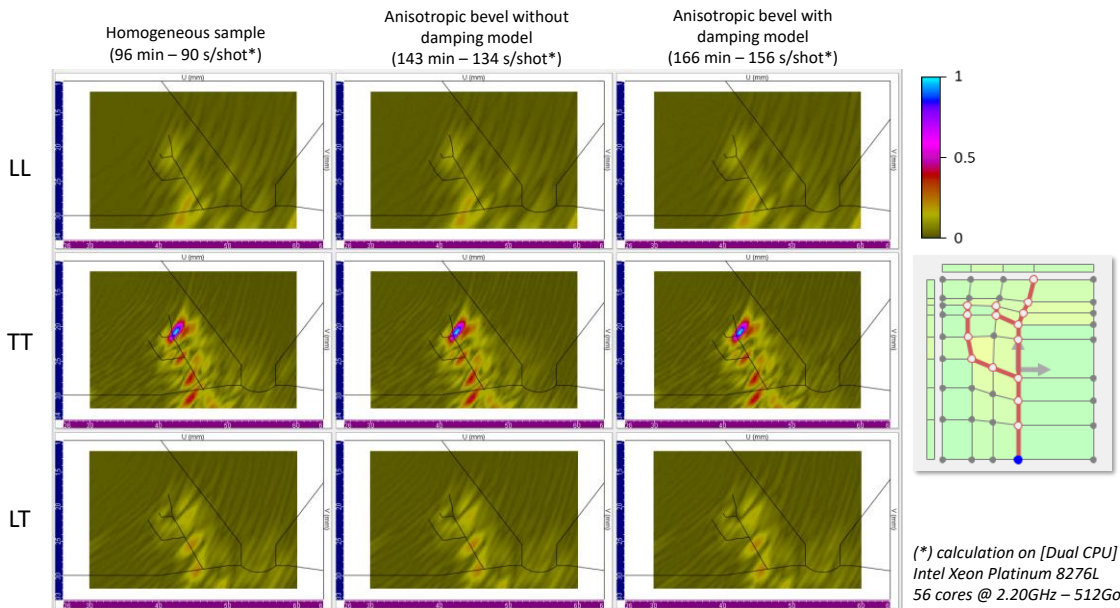


Figure 7: FE simulations of TFM imaging of a defect positioned before the bevel and comparisons considering three different descriptions for the weld material: on the left the homogeneous isotropic case, in the middle the MINA description without attenuation and on the right the same weld properties with attenuation accounted for.

As shown in Figure 7, when the crack is positioned before the bevel, the bevel material properties has virtually no influence on the simulated imaging results. Of course, the elementary A-scans are slightly different, but for acquisition times greater than the times of predominant indication values associated with the crack. Once the TFM imaging algorithm based on a time-of-flight cartography in a homogeneous part is applied, the differences according to the description of the weld material properties are negligible. Since calculation times increase with the complexity of the model describing the weld and therefore of the FE scheme used for the simulations, it seems sufficient, for a defect located before the weld, to consider a simple homogeneous medium. While this observation is relevant for a defect position before the bevel, it should be no longer the case if the defect position is chose into the weld.

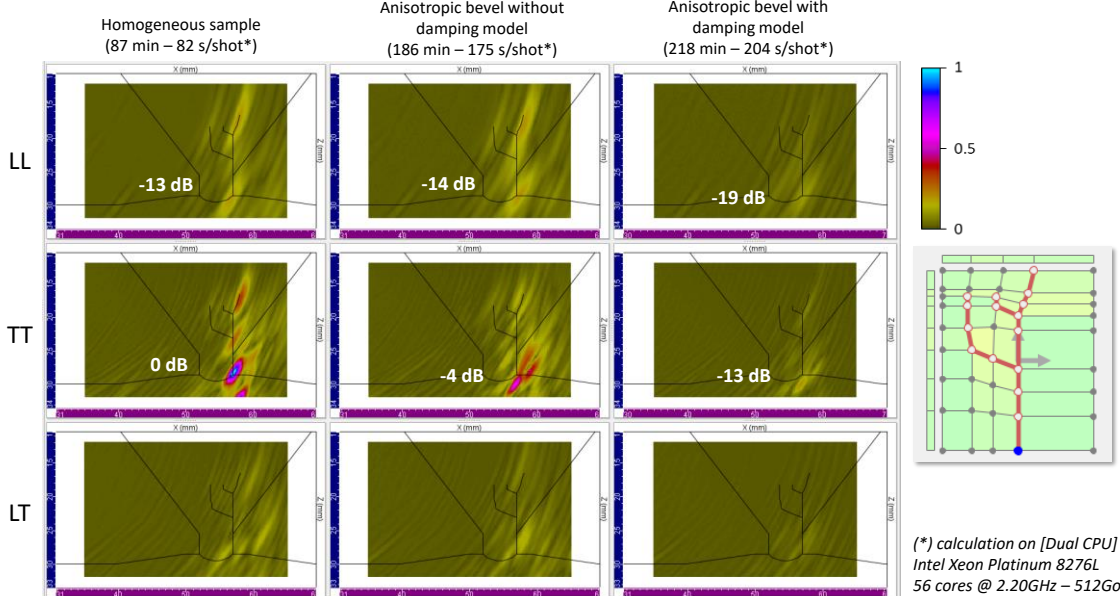


Figure 8: FE simulations of TFM imaging of a defect positioned on the left side of the bevel and comparisons considering three different descriptions for the weld material: on the left the homogeneous isotropic case, in the middle the MINA description without attenuation and on the right the same weld properties with attenuation accounted for.

In a second case, we are still comparing the influence of the properties of the weld material, but this time for a defect located on the right-hand side of the weld root (see Figure 8). The effects of the weld properties are then clearly visible. Without taking attenuation into account, we observe a drop in the amplitude of the indications that is solely linked to the inhomogeneous anisotropic properties of the weld. This corresponds to a kind of defocusing linked to the assumptions used to calculate the times of flight used for TFM imaging. It is worth emphasizing that this loss is much more noticeable for T waves (-4 dB for TT mode compared with -1 dB for LL mode). These losses are much greater when attenuation is taken into account in the propagation model (-5 dB and -9 dB for LL and TT modes resp.). This result is quite expected since the scattering phenomena at a fixed frequency are much more significant for T waves than for L. Thus, with the help of simulation, we quantify the performance losses due to diffusion phenomena in the microstructured part while guaranteeing a complete solution thanks to the use of fast FE models.

## 5. Conclusion

In view of the growing interest in advanced PAUT inspection methods for welded components, new features have been added to the CIVA simulation platform concerning weld description and new UT simulation tools. Two important points were discussed. The first concerns the various means used to help the user define the welded zone, both in terms of its geometry and the associated elastic properties. The other aspect concerns the need for simulated reference solutions for this type of components in order to overcome, if necessary, the limitations of HF propagation models or diffraction models on complex defects. The main challenge has been to efficiently control and automate the meshing and coupling procedures for the variety of cases allowed depending on various factors such as weld bevel and cracks geometries or probe position. The capabilities of the new FE module were demonstrated through short examples of simulated TFM imaging results. Other representative applications of the PAUT inspection simulation can already be carried out to compare this reference solution with other approximate CIVA models, highlighting all the advantages of this new approach.

Overall, the continued development and use of these advanced simulation tools offers great potential for improving inspection methods and gaining a better understanding of the phenomena induced by the presence of welds. The future challenges involve accelerating computations, especially in 3D, through innovative coupling techniques that accommodate variations in crack geometry and orientation.

## References

- [1] P. D. Wilcox, C. Holmes, and B. W. Drinkwater, "Advanced Reflector Characterization with Ultrasonic Phased Arrays in NDE Applications," *IEEE Trans. Ultrason. Ferroelectr. Freq. Control*, vol. 54, no. 8, pp. 1541–1550, Aug. 2007, doi: 10.1109/TUFFC.2007.424.
- [2] L. Le Jeune, S. Robert, E. Lopez Villaverde, and C. Prada, "Plane Wave Imaging for ultrasonic non-destructive testing: Generalization to multimodal imaging," *Ultrasonics*, vol. 64, pp. 128–138, Jan. 2016, doi: 10.1016/j.ultras.2015.08.008.
- [3] B. Chapuis, P. Calmon, and F. Jenson, *Best Practices for the Use of Simulation in POD Curves Estimation*. in IIW Collection. Cham: Springer International Publishing, 2018. doi: 10.1007/978-3-319-62659-8.
- [4] B. Puel, D. Lesselier, S. Chatillon, and P. Calmon, "Optimization of ultrasonic arrays design and setting using a differential evolution," *NDT E Int.*, vol. 44, no. 8, pp. 797–803, Dec. 2011, doi: 10.1016/j.ndteint.2011.08.008.
- [5] F. Dupont-Marillia, M. Jahazi, S. Lafreniere, and P. Belanger, "Design and optimisation of a phased array transducer for ultrasonic inspection of large forged steel ingots," *NDT E Int.*, vol. 103, pp. 119–129, Apr. 2019, doi: 10.1016/j.ndteint.2019.02.007.

- [6] J. Moysan, G. Corneloup, B. Chassignole, C. Gueudré, and M. A. Ploix, “Modelling welded material for ultrasonic testing using MINA: Theory and applications,” *AIP Conf. Proc.*, vol. 1430, no. 1, pp. 1219–1226, May 2012, doi: 10.1063/1.4716358.
- [7] K. Jezzine, A. Gardahaut, N. Leymarie, and S. Chatillon, “Evaluation of ray-based methods for the simulation of UT welds inspection,” *AIP Conf. Proc.*, vol. 1511, no. 1, pp. 1073–1080, Jan. 2013, doi: 10.1063/1.4789162.
- [8] A. Gardahaut, K. Jezzine, and D. Cassereau, “Paraxial ray-tracing approach for the simulation of ultrasonic inspection of welds,” *AIP Conf. Proc.*, vol. 1581, no. 1, pp. 529–536, Feb. 2014, doi: 10.1063/1.4864865.
- [9] B. Chassignole, P. Recolin, N. Leymarie, C. Gueudré, P. Guy, and D. Elbaz, “Study of ultrasonic characterization and propagation in austenitic welds: The MOSAICS project,” *AIP Conf. Proc.*, vol. 1650, no. 1, pp. 1486–1495, Mar. 2015, doi: 10.1063/1.4914766.
- [10] P. Guy, B. Mascaro, M. Darmon, N. Leymarie, and B. Clausse, “Accurate experimental determination of the complex elastic tensor of anisotropic materials of unknown orientation using ultrasonic transmitted bulk waves,” in *2019 International Congress on Ultrasonics*, Bruges, Belgium, Sep. 2019. Accessed: May 25, 2021. [Online]. Available: <https://hal.archives-ouvertes.fr/hal-02316999>
- [11] A. Lhémy, P. Calmon, S. Chatillon, and N. Gengembre, “Modeling of ultrasonic fields radiated by contact transducer in a component of irregular surface,” *Ultrasonics*, vol. 40, no. 1, pp. 231–236, May 2002, doi: 10.1016/S0041-624X(02)00143-9.
- [12] S.ourniac, N. Leymarie, N. Dominguez, and C. Potel, “Simulation of ultrasonic inspection of composite using bulk waves: Application to curved components,” in *Journal of Physics: Conference Series*, 2011, p. 012022. doi: 10.1088/1742-6596/269/1/012022.
- [13] K. Jezzine, A. Gardahaut, N. Leymarie, and S. Chatillon, “Evaluation of ray-based methods for the simulation of UT welds inspection,” *AIP Conf. Proc.*, vol. 1511, no. 1, pp. 1073–1080, Jan. 2013, doi: 10.1063/1.4789162.
- [14] D. Komatitsch and J. Tromp, “Introduction to the spectral element method for three-dimensional seismic wave propagation,” *Geophys. J. Int.*, vol. 139, no. 3, pp. 806–822, Dec. 1999, doi: 10.1046/j.1365-246x.1999.00967.x.
- [15] A. Imperiale and E. Demaldent, “A macro-element strategy based upon spectral finite elements and mortar elements for transient wave propagation modeling. Application to ultrasonic testing of laminate composite materials,” *Int. J. Numer. Methods Eng.*, vol. 119, no. 10, pp. 964–990, 2019, doi: 10.1002/nme.6080.
- [16] O. Mesnil, A. Imperiale, E. Demaldent, and B. Chapuis, “Validation of spectral finite element simulation tools dedicated to guided wave based structure health monitoring,” *AIP Conf. Proc.*, vol. 2102, no. 1, p. 050018, May 2019, doi: 10.1063/1.5099784.
- [17] A. Imperiale, N. Leymarie, T. Fortuna, and E. Demaldent, “Coupling Strategies Between Asymptotic and Numerical Models with Application to Ultrasonic Non-Destructive Testing of Surface Flaws,” *J. Theor. Comput. Acoust.*, vol. 27, no. 02, p. 1850052, Oct. 2018, doi: 10.1142/S2591728518500524.
- [18] A. Imperiale, N. Leymarie, and E. Demaldent, “Numerical modeling of wave propagation in anisotropic viscoelastic laminated materials in transient regime: Application to modeling ultrasonic testing of composite structures,” *Int. J. Numer. Methods Eng.*, vol. 121, no. 15, pp. 3300–3338, 2020, doi: 10.1002/nme.6359.